

Document downloaded from:

<http://hdl.handle.net/10251/103724>

This paper must be cited as:

López, JJ.; Molina, S.; García Martínez, A.; Valero-Marco, J.; Justet, F. (2017). Analysis of the potential of a new automotive two-stroke gasoline engine able to operate in spark ignition and controlled autoignition combustion modes. *Applied Thermal Engineering*. 126:834-847. doi:10.1016/j.applthermaleng.2017.07.213



The final publication is available at

<http://dx.doi.org/10.1016/j.applthermaleng.2017.07.213>

Copyright Elsevier

Additional Information

Analysis of the potential of a new automotive two-stroke gasoline engine able to operate in Spark Ignition and Controlled AutoIgnition combustion modes

J. Javier López^{a,*}, Santiago Molina^a, Antonio García^a, Jorge Valero-Marco^a,
Frédéric Justet^b

^a*CMT-Motores Térmicos
Universitat Politècnica de València
Camino de Vera, s/n. 46022 Valencia, SPAIN*
^b*Renault SAS
Technocentre
1, Avenue du Golf, 78288 Guyancourt, FRANCE*

Abstract

The need to reduce the emissions coming from automobiles encourages the attempts to study different engine configurations and new combustion strategies. In this case, a two stroke engine able to operate in Controlled AutoIgnition (CAI) and Spark Ignition (SI) combustion modes is studied, with the purpose of getting lower NO_x and CO_2 emissions than with other currently employed solutions. The engine configuration retained for the research is a uniflow scavenging configuration with intake ports in the cylinder liner and exhaust valves in the cylinder head. These valves are controlled by a Variable Valve Timing (VVT) system. The scavenging is guaranteed by an external blower driven by the crankshaft. Finally, the fuel supply is performed by a direct injection (DI) air-assisted fuel injection system.

*Corresponding author
Tel: +34 963 879 232. Fax: +34 963 877 659. E-mail: jolosan3@mot.upv.es

Through this paper the adjusting parameters to control the engine operation, as well as their influence on the CAI and SI combustion modes have been studied, providing the most relevant information and knowledge for controlling and optimizing the engine performance. Once these controlling parameters were studied, an EGR system was introduced in order to analyze the effect of this other parameter over the combustion process, as well as to determine the potential benefits of introducing such a system in this type of engines.

Keywords: Two-stroke engine, CAI, HCCI, Spark ignition, New combustion modes, Air-assisted injection

1. Introduction

Two stroke (2S) engines have always had their fashions, and these go on stage once in a while [1]. Traditionally, 2S engines had been cheaper than their competitors (four stroke -4S- engines), and also have had some advantages like less weight and more specific power, for example. But these engines also present some important troubles that hinders their development (scavenging difficulties, fresh air short-circuit, excessive thermal load on some components, etc.).

However, technological advances evolve and make now easy some tasks that were considered too complex a few years ago [2–4], giving room to solve the problems indicated before, which impede 2S engines development. Perhaps now it is a good time to reconsider the feasibility of this type of engines.

Additionally to this, nowadays engines have different ways to improve

15 their fuel efficiency [5]. A significantly promising way is CAI combustion
16 (Controlled AutoIgnition), where the combustion process is achieved by self-
17 ignition through the control of the temperature, pressure and composition
18 of a premixed charge, instead of the traditional spark ignition for gasoline
19 engines [6]. This is one of the most promising combustion technologies to
20 reduce fuel consumption and NO_x emissions in gasoline engines. Currently,
21 however, CAI combustion is constrained at part load operating conditions
22 because of misfire at low load and knocking combustion at high load.

23 Some additional benefits of the CAI combustion process, compared to
24 the traditional SI combustion process, is that it is more stable, thus getting
25 better repeatability of the combustion cycles, together with fewer misfires.
26 In Figure 1, an operating point at low load (2000 rpm with an IMEP -
27 Indicated Mean Effective Pressure- of around 3 bar) for the engine studied in
28 this work is presented in two graphs, where the equivalence ratio is varied to
29 obtain different combustion modes: on the left a spark ignition combustion
30 mode, whereas on the right a CAI mode. From the figure, it can be seen
31 that the standard deviation of the IMEP (σ IMEP) is much lower under
32 CAI conditions, thus achieving significant improvements in the combustion
33 process leading to lower fuel consumption. Besides, thanks to the different
34 combustion process, lower pollutant emissions compared to a traditional SI
35 combustion process are obtained [7].

36 Nevertheless, despite the attractive advantages underlined before, this
37 combustion mode has also got some limitations. On the one hand, the in-
38 cylinder pressure gradients tend to increase with the engine load, and CAI
39 gradually becomes knocking, which is harmful for the mechanical integrity of

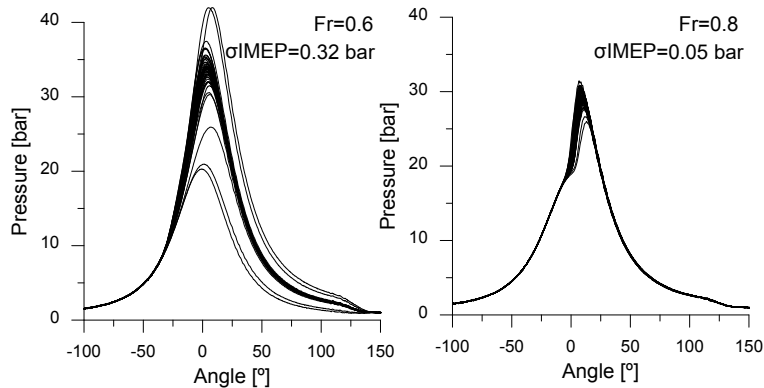


Figure 1: Same operating point (2000 rpm, IMEP \sim 3 bar) with different combustion modes. **Left.**- SI mode. **Right.**- CAI mode.

40 the engine, thus limiting the CAI operating range. On the other hand, the
 41 classical control of the combustion onset by the spark is lost, and the control
 42 of this type of combustion mode becomes a real challenge, since the autoigni-
 43 tion conditions are very sensitive to small changes in the engine operating
 44 conditions.

45 Looking back in time, CAI combustion technology was first applied suc-
 46 cessfully in 2S gasoline engines by Onishi et al. [8] and by Noguchi et al. [9].
 47 This particular combustion mode can be achieved more easily in 2S engines
 48 thanks to their operation singularities, since one of the main operation prin-
 49 ciples of CAI is to warm up the intake charge in order to increase the mixture
 50 reactivity [10], and this can be better done in 2S engines. In fact, in 4S en-
 51 gines, the intake and exhaust processes take place in two separate strokes,
 52 and the exhaust gases are almost completely scavenged from the cylinder,
 53 whereas in 2S engines these two strokes are substituted by a scavenging pro-
 54 cess, which is carried out around bottom dead center (BDC), allowing to

55 heat up the initial in-cylinder charge by “simply” controlling the amount of
56 hot residuals that remain in the cylinder. Some authors have tried to get
57 this effect in 4S engines making an exhaust re-breathing [11, 12], but they
58 faced two important problems: the significant complexity of the distribu-
59 tion system required to produce this effect, and the heat losses during the
60 re-breathing process.

61 The purpose of this paper is to present the potential of a new 2S gasoline
62 engine concept able to operate in SI and CAI combustion modes, which is
63 able to compete with current, more standard gasoline engines in terms of
64 fuel consumption for the same peak power and cost. This engine concept
65 can be applied either to emerging markets or to more stringent markets. In
66 the first case (emerging markets), the NO_x limit would be achieved without
67 any specific after-treatment system for this pollutant, making use of the
68 advantages of the CAI combustion in terms of NO_x emissions. In the second
69 case (more stringent markets), an EGR system will be required as a way to
70 fulfill the NO_x limit. In both scenarios, the traditional three way catalyst
71 used in gasoline engines will be removed to allow the operation under lean
72 mixture conditions, which would improve fuel efficiency. The only exhaust
73 after-treatment system that will be used is an oxidation catalyst, the use of
74 which is unavoidable in any premixed combustion engine to remove CO and
75 UHC emissions.

76 Throughout the whole paper, the influence of the different engine config-
77 urations and parameters on the two operating modes (SI and CAI), as well
78 as the transition between them, will be analyzed, showing at the same time
79 the results in terms of combustion performance, fuel consumption and NO_x

80 emissions.

81 The paper structure is as follows: the next section deals with the en-
82 gine configuration, how the experimental data is processed and which test-
83 ing methodology is used. Later, the main results of the current research are
84 presented in two parts: first, the engine behavior without EGR is shown,
85 focusing on the effect of the fuel/air ratio, the VVT position and the injec-
86 tion parameters; and, second, the effect on the combustion process of adding
87 EGR to all the previously analyzed parameters is studied. Finally, the main
88 conclusions of the study will be enunciated.

89 **2. Experimental facilities and methods**

90 In this section, the following information will be given:

- 91 • The description of the final engine configuration, as well as the main
92 reasons that justify the different selections.
- 93 • The test bench with the prototype engine (single-cylinder engine).
- 94 • Some details about the data processing, showing how the main param-
95 eters used in the analysis are determined.
- 96 • The testing methodology.

97 *2.1. Engine Configuration Selection*

98 The developed engine will be a 2S uniflow-scavenged twin-cylinder engine
99 with Variable Valve Actuation (VVA) and direct injection. Besides, it will be
100 a relatively small engine, with around 0.6 liters of total displacement volume,

101 suited for small vehicles. The main reasons behind the selection of the engine
102 configuration finally retained will be discussed in this subsection.

103 Since the most common configuration in 4S engines is overhead valves,
104 the first idea coming to mind is to keep this configuration to take advan-
105 tage of all the cumulated know-how about this way to design automotive
106 engines. However, 2S engines require a very high permeability because they
107 have much less time to perform the intake and exhaust processes, hence the
108 interest in the use of ports in these engines. Among the different possibilities,
109 the uniflow scavenging configuration with overhead poppet valves is chosen,
110 with intake ports and exhaust valves (Figure 2), since it is a widely employed
111 configuration in applications other than automotive, with extremely good re-
112 sults [13–16]. The scavenging quality is greater than in other configurations,
113 and permeability is much higher (at the intake by the incorporation of a high
114 number of ports along the cylinder periphery, and at the exhaust because the
115 space available in the cylinder head is greater, since there are only exhaust
116 valves, and they can be larger).

117 Among the different VVA systems, a Variable Valve Timing (VVT) sys-
118 tem has been considered to be installed in the camshaft actuating on the
119 exhaust valves, enabling the modification of its angular position (Figure 3).
120 In the figure and further on, the camshaft angular position is depicted by the
121 Exhaust Valve Closing (EVC). The selection of this system was made paying
122 attention to its cost. Such a system allows optimizing the scavenging process
123 at different engine speeds, as well as modifying the effective compression and
124 expansion strokes. It is important to note that with this system the valves
125 opening and closing will be modified at the same time, and the lift duration

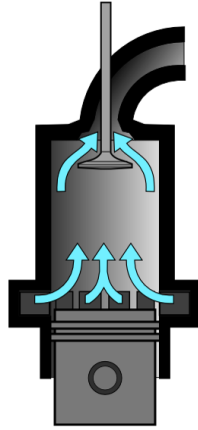


Figure 2: Uniflow scavenged engine (from Wikipedia.org).

126 will remain the same.

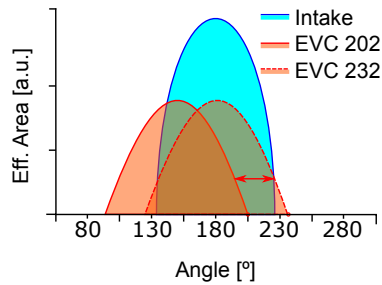


Figure 3: Distribution scheme where the two extreme positions of the VVT are shown.

127 Since the intake of the fresh air is not induced like in 4S engines, some
 128 scavenging pump is needed. To allow the maximum flexibility with a reason-
 129 able cost, a mechanical blower, driven by the crankshaft, will be used.

130 As in any 2S engine, air short-circuiting is unavoidable, and consequently
 131 it is strongly recommended to inject the fuel directly inside the combustion
 132 chamber once the ports and valves are already closed. Thus, a fuel direct
 133 injection system is required, but paying attention to the cost of the system,

134 finally an air-assisted fuel injection system will be retained. This system
 135 consists of two injectors: the first one introduces the gasoline inside a pres-
 136 surized chamber, filled with air, located just above the second injector. Later,
 137 this premixture is introduced in the cylinder (Figure 4). Such a system al-
 138 lows a good enough atomization without the need of high (and “expensive”)
 139 pressures.

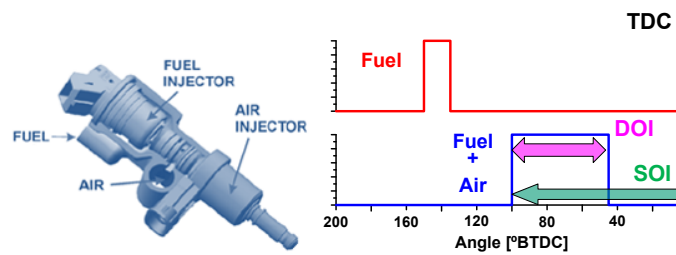


Figure 4: Air assisted injector sketch (left) and operation scheme (right).

140 The operating scheme shown in Figure 4 to the right, shows the preinjec-
 141 tion of the fuel inside the air injector and, after a prefixed delay, the injection
 142 of this premixture (air + fuel) inside the cylinder. The main parameters to
 143 be set are the following: the amount of fuel introduced, the starting angle of
 144 the premixture injection (SOI, Start Of Injection) and the duration of this
 145 injection (DOI, Duration Of Injection). With this last parameter (DOI), the
 146 amount of air injected together with the fuel can be modified.

147 2.2. Experimental facilities

148 Even if, as indicated before, the definitive engine will be a twin-cylinder
 149 engine, the engine used for the current research is a single-cylinder, prototype
 150 engine, with the same configuration as in the final twin-cylinder engine. This
 151 choice is very common in basic research activities, since a single-cylinder

152 engine enables a much better analysis of the obtained results. The intake
153 and exhaust lines of this single-cylinder engine have not been optimized from
154 the acoustic point of view because, anyway, all these phenomena will be
155 significantly different to those of the final (twin-cylinder) engine. However,
156 the exhaust system has got a controlled back-pressure to resemble the one
157 existing in the real engine, and some acoustic shock absorbers have been
158 installed in the intake and exhaust lines not to optimize but, at least, to
159 mitigate the possible adverse effects of the pressure waves.

160 The instrumentation installed in the engine and in the test cell to drive
161 and control the engine, and to extract the necessary data from it during
162 each test is as follows: an optical highly precise encoder is connected to the
163 crankshaft to know exactly its instantaneous position. The in-cylinder pres-
164 sure is measured twice with two piezoelectric sensors (Kistler 6061B U20).
165 This redundant measurement is done to be sure about the proper operation
166 of these key and critical sensors. To get a reference for the in-cylinder pres-
167 sure, a piezo-resistive pressure sensor was installed in the liner near BDC
168 (Kistler 4007B).

169 The single-cylinder engine can't run by itself, since many of the elements
170 available in the real and definitive engine are not mounted on it. These
171 missing elements need to be installed in the test cell, a complete sketch of
172 which can be seen in Figure 5:

- 173 • The dry sump lubrication system as well as the cooling system are
174 externally assisted with pressure, flow and temperature control.
- 175 • The intake system has got an external screw compressor to emulate the
176 effect of the mechanical blower from the real engine. In this facility the

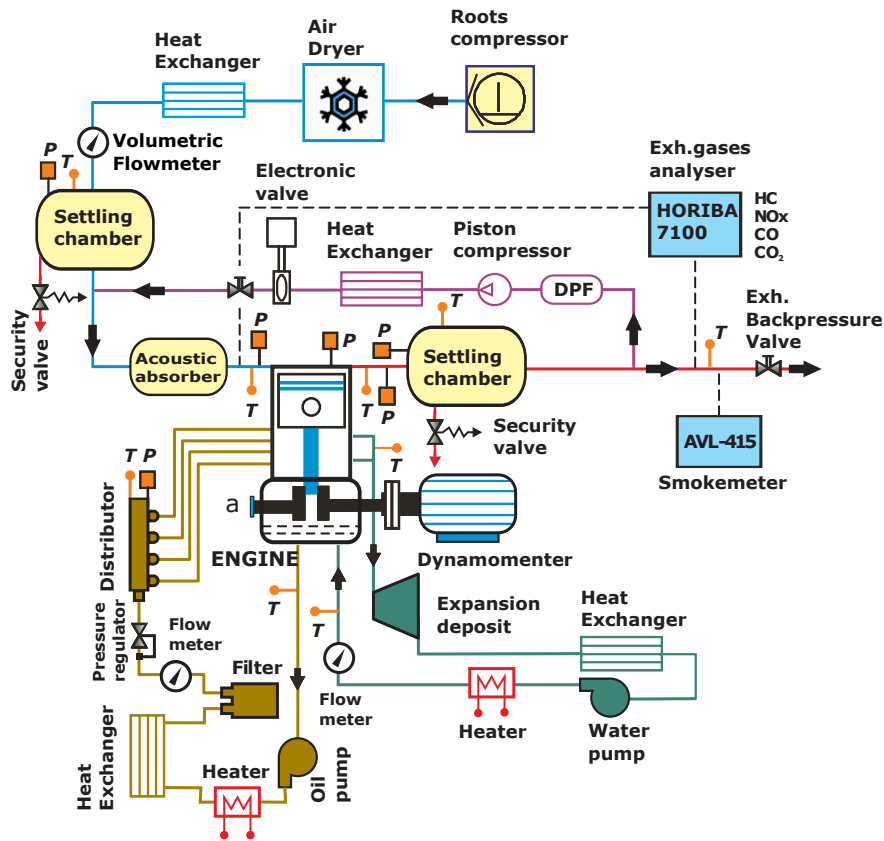


Figure 5: Test cell sketch.

177 temperature, humidity, pressure, mass flow and chemical composition
 178 (EGR) of the gas are controlled.

- 179 • In the exhaust line a pneumatically-controlled valve is used to control
 180 the backpressure, maintaining its value to that equivalent in the real
 181 engine.
- 182 • The EGR (External Gas Recirculation) facility is an external, low pres-
 183 sure system. It has got a particulate filter to suppress the soot particles,

184 a cooling system, a compressor, and a flow regulator, controlled by the
185 CO_2 content of the intake gases, so as to control the EGR rate.

186 Finally, the fuel mass consumption is measured by a Horiba FQ2100 de-
187 vice, which is suitably adapted for small consumptions (it is important to
188 keep in mind that the engine is a small, single-cylinder engine), and the
189 exhaust gases composition is measured by a Horiba MEXA 7100.

190 *2.3. Data processing*

191 In this subsection, how the main parameters, later used in the analysis,
192 are deduced from the experimental measurements is described.

193 *2.3.1. BSFC estimation*

194 The single-cylinder prototype engine used in this research is far from the
195 real engine in many aspects. For example, it has not a mechanical blower
196 driven by the crankshaft (the real engine needs to have one), and it has two
197 counter-rotating balance shafts for inertia compensation (these will not be
198 used in the real engine), leading to a set of mechanical losses that are not
199 representative of the real engine. Despite these differences, it is important
200 to estimate the main engine parameters for the real engine, in such a way
201 that these parameters are more fair and useful for comparison. For this
202 reason, the BMEP (Brake Mean Effective Pressure) is estimated from the
203 IMEP (Indicated Mean Effective Pressure) taking into account the following
204 mechanical losses:

- 205 • The friction losses + driving power of the water pump, using a suitable
206 correlation as a function of the engine speed.

207 • The work performed by the mechanical blower supplying the intake air,
208 using an experimental correlation after testing the real blower.

209 • The work performed by the high pressure compressor supplying the air
210 for the fuel injection system, using an experimental correlation after
211 testing the real compressor.

212 After considering all these losses, the BMEP and, thus, the BSFC of the
213 twin-cylinder engine can be properly estimated.

214 *2.3.2. IGR estimation*

215 The IGR (Internal Gas Recirculation) is the amount of residual hot gases
216 remaining inside the cylinder after the gas exchange process is over. To cal-
217 culate this parameter, first, it is necessary to know the fresh charge amount
218 (i.e. air + EGR gases) trapped in the cylinder, which is measured by in-
219 jecting methane in the intake manifold (as a gas tracer), and measuring its
220 content in the exhaust, as described in [17]. This allows computing the trap-
221 ping ratio or trapping efficiency. Once this is known, the trapped residual
222 gases are estimated with the equation of state and an in-cylinder enthalpy
223 balance at the beginning of the compression process (also described in [17]),
224 with the following assumptions: the trapped air is assumed to have the tem-
225 perature measured in the intake manifold (i.e. around the intake ports) and
226 its quantity is known thanks to the trapping ratio determined previously;
227 the residual gases temperature is calculated from the temperature measured
228 in the exhaust manifold, taking into account the possible amount of short-
229 circuited fresh charge; the in-cylinder pressure is assumed to be the one
230 measured in the cylinder at the corresponding crank angle. To have this last

231 information, as already mentioned above, a piezo-resistive pressure sensor
232 was installed near BDC, to be able to measure this pressure. Finally, with
233 the two equations mentioned above, the mass of residuals is determined.

234 *2.3.3. Other parameters*

235 **EGR rate measurement**

236 The measurement of the EGR rate is performed based on the CO_2 content
237 in the intake and in the exhaust gases. With this twofold measurement, the
238 EGR content in the intake charge can be determined.

239 **Heat Release Rate (HRR)**

240 The HRR's are calculated by the in-house code Calmec [18, 19] using a
241 classical procedure, which makes use of the instantaneous in-cylinder pres-
242 sure, applying the first law of Thermodynamics and a heat losses model based
243 on the Woschni equation.

244 **Knock detection**

245 The MAPO (Maximum Amplitude of Pressure Oscillations) parameter
246 is the one selected to detect knock, which is based on the analysis of the
247 high frequency amplitudes in the in-cylinder pressure signal [20]. To obtain
248 the MAPO, the raw pressure signal is band-pass filtered (between 5 and
249 20 kHz), and the maximum amplitude of the resulting signal is taken. When
250 the MAPO value surpasses a given limit, knock is considered to occur. The
251 MAPO limit is considered to depend linearly with the engine speed, being
252 1.8 bar at 2000 rpm and 3.8 bar at 4000 rpm (these values were determined
253 by in-house experience). Finally, it is worthy to underline that the MAPO
254 parameter is checked on-line for engine surveillance when performing the
255 different tests.

256 **Estimated performance in standard cycles**

257 Among the different results shown in this research, the performance of
258 the engine, mounted on a vehicle, in some standard cycles will be given. To
259 perform this estimation, a group of operating points spread all along the en-
260 gine operating map are selected, and they are tested in the engine test bench.
261 Later, with the information available on each of these points, the main en-
262 gine parameters (e.g. BSFC, BSNO_x, etc.) are estimated on the whole engine
263 map by interpolation/extrapolation. Finally, with all this information, the
264 results for any given standard cycle can be predicted. Another additional
265 data important to perform the prediction is the vehicle mass (700 kg), the
266 engine peak power (30 kW) and the gearbox definition, which has been opti-
267 mized to minimize NO_x emissions in the Bharat cycle. The standard cycles
268 considered in the frame of this work are Bharat (currently in force in India),
269 NEDC (New European Driving Cycle) and WLTP (Worldwide harmonized
270 Light vehicles Test Procedure).

271 *2.4. Testing methodology*

272 For this study, each operating point is defined by an engine speed and a
273 given fuel mass. There are two main reasons for choosing the fuel mass as
274 an indicator of the engine load, instead of the BMEP: first, because BMEP
275 is not a direct measurement, and consequently doing tests at a given BMEP
276 would take a lot of time and effort; and, second, because in 2S engines the en-
277 gine behavior depends quite a lot on the combustion characteristics (strongly
278 dependent on the fuel mass), since it significantly affects the scavenging pro-
279 cess. Consequently, changing the fuel mass in equivalent operating points
280 would complicate the comparison. However, when presenting the results, an

281 illustrative value of the IMEP will be given, at each operating point, as a
282 reference of the engine load (please note that the corresponding IMEP of an
283 equivalent 4S engine will be approximately twofold).

284 Once the test point is defined (engine speed and fuel mass), the following
285 degrees of freedom are explored to see which influence they have on the
286 combustion process:

- 287 • Equivalence ratio (Fr): This parameter is adjusted by modifying the
288 amount of air introduced in the engine (since the fuel mass flow is fixed
289 for a given operating point). This equivalence ratio is calculated from
290 the measured engine flows (air -including the injected air- and fuel),
291 and it is equivalent to the one that can be measured in the exhaust by
292 the exhaust gas analyzer.
- 293 • EVC position, which can be adjusted between 202° and 232° .
- 294 • Injection parameters: SOI and DOI (referred to the direct injection
295 event, i.e. the air + fuel injection). To select these two parameters,
296 attention should be paid to the in-cylinder pressure at EOI (End Of
297 Injection), to guarantee that the injection pressure is above this other
298 pressure during the whole injection event. In fact, the EOI is limited to
299 40 to 50° BTDC (Before TDC), depending on the operating conditions.
- 300 • The spark timing. Under SI operating mode, this parameter is intended
301 to be placed at MBT (Maximum Brake Torque), even if, usually, this
302 location is unachievable because of knock.
- 303 • The EGR rate.

304 Finally, each test has two sets of measurements: instantaneous and mean
305 measurements. For the instantaneous ones, 250 consecutive cycles are recorded,
306 and for the mean ones the averaging time is 60 seconds.

307 **3. Results and discussion**

308 The presentation of the results will be as follows. First, the peculiarity of
309 this engine, regarding its ability to operate in different combustion modes,
310 will be presented. On a next step, the effect of the Fr (fuel/air equivalence
311 ratio) and VVT position will be reviewed, as well as the effect of the injection
312 settings (SOI and DOI, in both cases referred to the direct injection of the
313 fuel + air mixture), trying to summarize the results already presented in two
314 previous publications [21, 22]. Finally, as a new contribution of the present
315 paper, the effect of using EGR on the performance of this engine will be
316 analyzed.

317 *3.1. The different combustion possibilities of this engine*

318 Because of its characteristics, this engine can operate in two different
319 combustion modes: SI and CAI. And recently it has been proven that it can
320 switch from one mode to the other without any trouble [23]. The operation
321 in one or the other mode mainly depends on the IGR ratio and the initial
322 temperature of the in-cylinder charge. In fact, both parameters are strongly
323 affected by the engine load, as illustrated qualitatively in Figure 6. As far
324 as the engine load is reduced, the amount of air required by the engine is
325 lower, and the scavenging process is less efficient, thus explaining why the
326 IGR ratio increases. Regarding the initial temperature of the in-cylinder
327 charge, it is the result of an enthalpy balance between the fresh charge (at

328 the intake temperature) and the IGR gases (at the exhaust temperature in
 329 a first approach). The increase in IGR ratio as far as the engine load is
 330 reduced explains why the initial temperature of the charge increases initially.
 331 But at very low loads, this trend is reversed, which is justified by the decrease
 332 in exhaust temperature (i.e. the temperature of the IGR gases) due to the
 333 decreasing fuel mass burnt.

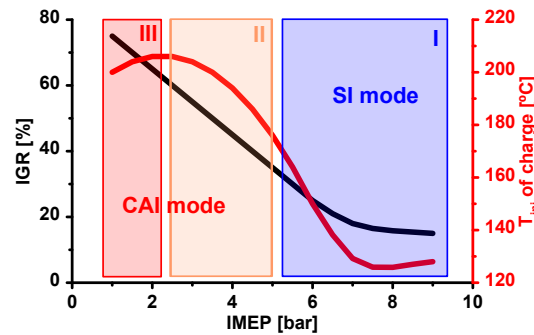


Figure 6: Evolution of the IGR ratio and the initial temperature of the in-cylinder charge with the engine load.

334 Based on the above explanation, three different regions have been indi-
 335 cated in Figure 6:

- 336 • Region I: at high loads, where the IGR and the initial temperature of
 337 the charge are moderate, the combustion process is controlled by the
 338 spark, as in any conventional SI engine. In this scenario, the autoigni-
 339 tion of the mixture is dangerous for the mechanical integrity of the
 340 engine (knock), and consequently it needs to be avoided.
- 341 • Region III: at low loads, the fuel burns in purely controlled autoignition
 342 (CAI) mode because of the enhanced reactivity of the in-cylinder charge

343 caused by its high temperature (this is demonstrated in Appendix A).
344 This CAI operation mode introduces some advantages that will be fur-
345 ther discussed later: increased engine stability (as already shown in the
346 introduction, see Figure 1), misfiring avoidance (which commonly takes
347 place in engines operating with high percentages of residual gases), low
348 NO_x , etc.

- 349 • Region II: between the two previous regions, at medium loads, a tran-
350 sition between SI and CAI takes place.

351 Because all these three scenarios are significantly different, they will be
352 analyzed separately in the upcoming subsections. The operating points se-
353 lected to present and analyze the results are shown in Figure 7. Point 1,
354 at maximum torque, has been taken as representative for region I because
355 of its importance in the engine map. Points 2a and 2b have been taken as
356 representative for region II, and Point 3 for region III. These points were
357 selected because of their relevancy in the standard cycles.

358 Finally, it is important to point out that the data used to present the
359 results were selected trying to better show the effect of the analyzed param-
360 eters, and consequently they do not necessarily correspond to the best results
361 obtained with the engine.

362 Now the influence of the different engine settings on the combustion pro-
363 cess will be analyzed.

364 3.2. *Effect of Fr and VVT position*

365 In 2S engines, the in-cylinder trapped gas composition at the beginning
366 of the compression stroke can be very different depending on the scavenging

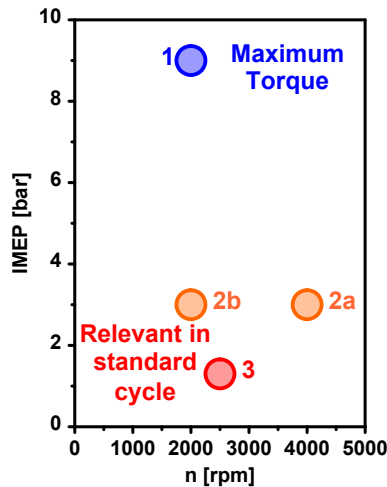


Figure 7: Selected points to present and analyze the results.

367 process. This gives further implications to the effect of the equivalence ratio
 368 and the VVT position at each operating point, compared to what would
 369 happen in 4S engines.

370 Now, taking into account the description shown in section 3.1, the results
 371 will be structured in the different combustion modes presented there.

372 3.2.1. High load – SI mode

373 At high loads the engine works like any SI engine. At these conditions,
 374 the autoignition of the charge is not controllable, and the corresponding
 375 pressure oscillations can damage the engine integrity. Thus, under these cir-
 376 cumstances, the autoignition is considered as knock, and needs to be avoided.

377 In a high load operating point, like the one under analysis now, usually
 378 pollutant emissions are not a big concern, since it is outside of the usable
 379 region during the standard cycle. Consequently, the most important param-
 380 eter for the analysis in the present conditions is the fuel efficiency, that can

381 be quantified by the BSFC. Figure 8 shows that BSFC correlates well with
 382 the CA75 angle (Crank Angle where 75% of the fuel mass has been burned),
 383 getting better fuel consumptions with earlier positions of the CA75. The
 384 different points in the figure correspond to different EVC's and Fr's, and the
 385 spark timing has been set for each case up to reach the MBT (Maximum
 386 Brake Torque) without exceeding the knock limit. Based on the figure, the
 387 CA75 seems to be the key parameter to understand how BSFC can be op-
 388 timized, since it combines the combustion phasing -CA50- and its duration:
 389 what is important is to have, at the same time, a fast combustion (i.e. short
 390 duration) and a well-phased combustion (i.e. a small CA50), and this twofold
 391 information is suitably summarized in the CA75 parameter.

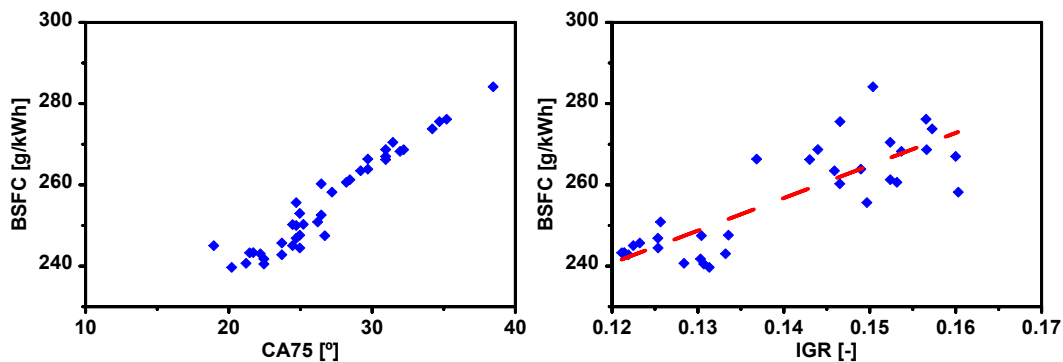


Figure 8: **Left.-** Evolution of BSFC with CA75 at Point 1. **Right.-** For the same tests, correlation between BSFC and IGR ratio.

392 The start of combustion is very important to advance the CA75 and get
 393 better fuel consumption. In the case of a spark controlled operating point, as
 394 the one under analysis now, this start of combustion is controlled by the spark
 395 timing, which should be commanded earlier to improve BSFC. However, the
 396 appearance of knock limits the spark timing advance, thus limiting BSFC.

397 The result shown in Figure 8 seems to indicate that something might change
398 in the engine when either Fr and/or EVC are modified. With the aim of
399 finding an explanation to this behavior, Figure 8 was built, showing that
400 BSFC is also well correlated with the IGR rate: as the IGR rate decreases, the
401 fuel efficiency is improved. An increase in IGR rate has two opposed effects:
402 on the one hand, the temperature of the charge is increased thus increasing
403 the mixture reactivity; but, on the other hand, the oxygen content is reduced,
404 thus reducing the mixture reactivity. Appendix A shows some calculations
405 made with Chemkin in order to evaluate the autoignition delay of a mixture
406 composed by fresh air and IGR. As a conclusion, for moderate IGR rates the
407 effect of the temperature increment is stronger than the oxygen reduction,
408 and consequently it can be said that the mixture reactivity increases with
409 an increase in IGR rate. The results shown in Figures 8 and 8, then, can be
410 interpreted as follows: BSFC is improved when the IGR rate is reduced, and
411 this is because the mixture reactivity is reduced, which avoids the appearance
412 of knock and allows an earlier spark timing and, consequently, an earlier
413 CA75.

414 Therefore, at high loads, where the engine works in SI mode, the appro-
415 priate configuration of the VVT and Fr will be the one that minimizes the
416 amount of IGR.

417 *3.2.2. Mid-load – SI / CAI transition*

418 As far as the engine load is decreased, the amount of fuel to burn is smaller
419 and the IGR rates are higher, leading to higher dilution of the in-cylinder
420 charge. Thus, pressure gradients generated by the combustion and autoigni-
421 tion processes become more controllable and admissible for the engine.

422 At these operating conditions CAI combustion starts to be an option
 423 to operate the engine. The transition between the SI and CAI combustion
 424 modes is based on the control of the mixture reactivity by means of the IGR
 425 rate modification. In Figures 9 and 10, the transition between both modes is
 426 shown with an Fr variation. In view of these results the following comments
 427 can be introduced:

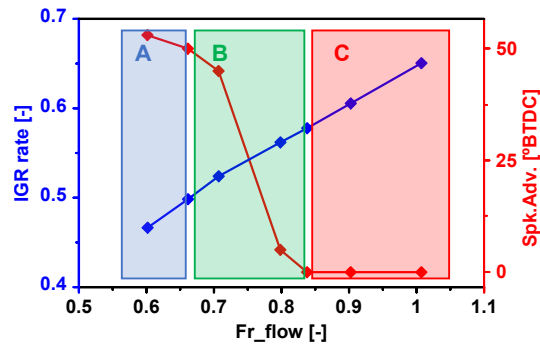


Figure 9: Transition from SI to CAI conditions at Point 2a.

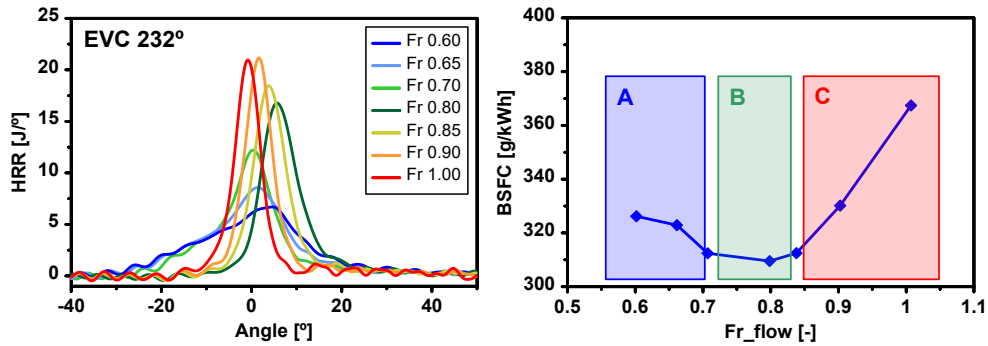


Figure 10: **Left.-** Effect of Fr on the HRR at Point 2a. **Right.-** Effect of Fr on BSFC for the same conditions. The tests are the same as in Figure 9.

- 428 • At low Fr (region A) the mixture reactivity is not enough to reach stable
 429 autoignition conditions. Under these conditions the combustion needs

430 to be initiated by the spark, and the spark timing should be commanded
431 early enough to get a stable and well centered combustion.

432 • At high Fr (region C) the mixture reactivity is much higher, and the
433 autoignition conditions are reached. The spark ignition control is lost
434 (in fact, the spark event could be even removed), the combustion pro-
435 cess is much faster (narrower HRR) and it starts to be placed too early,
436 thus penalizing BSFC (as shown in Figure 10).

437 • Finally, at region B, placed between the two previously explained cases,
438 there is an optimum value for Fr where the mixture reactivity is the
439 best suited. For this particular value of Fr the combustion process is,
440 at the same time, fast and well located in the cycle, and consequently
441 the BSFC reaches a minimum value.

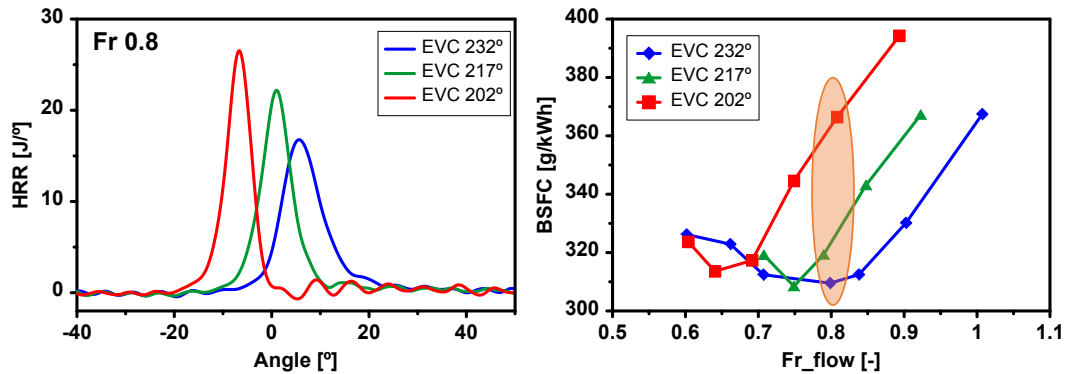


Figure 11: Effect of VVT on the HRR (left) and BSFC (right) at Point 2a operating in CAI mode.

442 Once the combustion control by the spark is lost (regions B and C), it can
443 be recovered by the VVT position, as illustrated in Figure 11. This effect is

444 because of the influence of the VVT position on the scavenging process and
 445 on the in-cylinder thermodynamical conditions (see Figure 12). An early
 446 VVT position, for instance (e.g. EVC 202°), leads to a reduced effective
 447 expansion stroke and, thus, a higher exhaust temperature. This means that
 448 the IGR gases will be hotter. At the same time, this early VVT position will
 449 increase the effective compression ratio (which is defined as the ratio between
 450 the volume in the cylinder when the exhaust valves are closed and the one
 451 when the piston is at TDC), as demonstrated by the in-cylinder pressure at
 452 -40° ATDC shown in the figure. Both effects (hotter IGR and higher effective
 453 compression ratio) would lead to a much reactive mixture, thus explaining
 454 the trend observed in Figure 11.

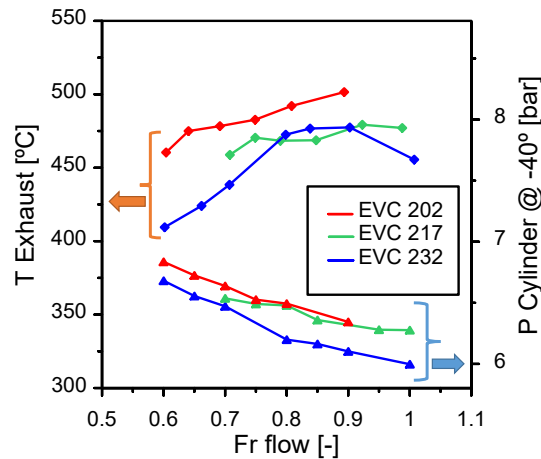


Figure 12: Exhaust temperature and in-cylinder pressure -40° ATDC for all the cases presented in Figure 11.

3.2.3. Low load – “Pure” CAI mode

455 At low load conditions, the IGR rate is well above 50% (i.e. the residual
 456 gases mass is bigger than that of the fresh air). These IGR rates lead to
 457

458 a significantly high temperature in the in-cylinder charge together with an
 459 extremely low oxygen concentration. Such a mixture may present difficulties
 460 for being ignited by a spark, but can autoignite with no danger for the engine
 461 mechanical integrity. Thus, at these conditions, the control of the combustion
 462 onset by the spark is completely lost. This is shown in Figure 13, where a
 463 wide swept of spark timings has been performed, including an extra case
 464 with no spark ignition, at the operating conditions corresponding to Point
 465 3 (see Figure 7). It can be observed that the combustion process is not
 466 affected by the spark timing, nor by the spark ignition, at all. The only role
 467 of the spark under these conditions is just to start the engine and to hold the
 468 combustion process when the engine is still cold. And, as indicated before,
 469 the combustion onset can be controlled with the parameters that control the
 470 mixture reactivity, namely Fr and VVT position.

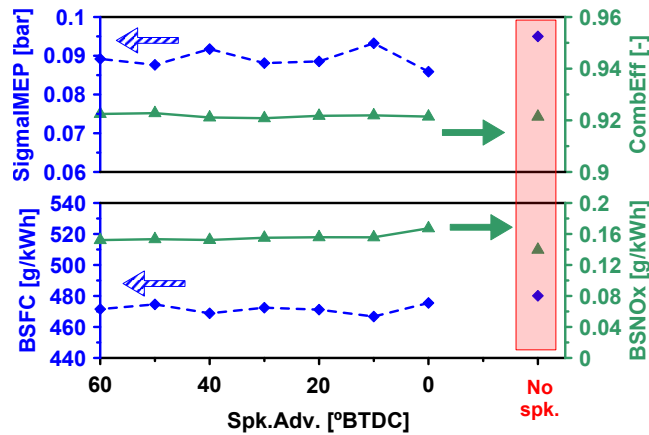


Figure 13: Effect of the spark timing on different engine outputs at Point 3.

471 Finally, two additional remarks from the previous figure: at these con-
 472 ditions the NO_x emissions are extremely low (below 0.2 g/kWh), which is

473 due to the low combustion temperatures (mainly because of the very low
474 initial oxygen concentration in the in-cylinder charge), and the engine stabil-
475 ity is outstanding ($\sigma IMEP$ below 0.1 bar), which is a typical characteristic
476 associated to the CAI combustion mode, as indicated in the introduction
477 section.

478 3.3. Effect of the injection parameters (SOI-DOI)

479 In section 2.1 the fuel injection system was described. It is an air-assisted
480 direct injection system, where the start of injection (SOI) and its duration
481 (DOI) can be adjusted. It is worthy to remind here that both SOI and DOI
482 refer to the air+fuel injection process. As already said before, for a given
483 operating point the fuel amount is prefixed, and a modification of the DOI
484 affects the air quantity injected together with the fuel.

485 On the one hand, based on the analysis of all the available results, it
486 can be said that, in general, an advanced SOI helps to improve the combus-
487 tion process, since the time available to homogenize the mixture is higher.
488 However, when the engine load is reduced, this trend is not always observed
489 (see Figure 14). A possible explanation could be that, for advanced SOI's,
490 the fuel is excessively spread in the IGR gases (please note that a reduction
491 in the engine load considerably increases the IGR rate, see Figure 6), thus
492 hindering the ignition of the mixture.

493 As a conclusion, regarding the effect of the SOI, unfortunately there is not
494 a well defined general trend linking this parameter with the correct engine
495 operation for all the tested points.

496 On the other hand, the effect of the DOI on the combustion process shows
497 that there is an optimal value for this parameter that depends on the engine

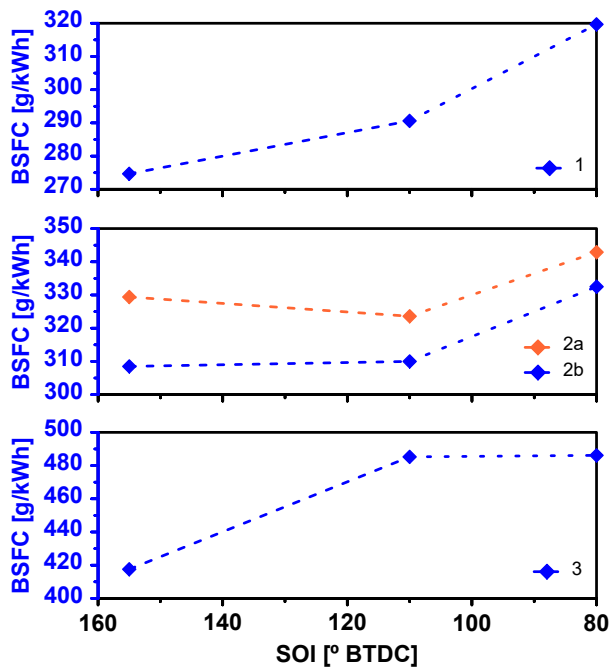


Figure 14: Effect of SOI on BSFC at high (**top**), mid (**center**) and low load (**bottom**).

498 speed and load. The key parameter to analyze the relationship between the
 499 DOI and the combustion behavior is the IAR (Injected Air Ratio)[22], which
 500 relates the injected air mass with the total air mass trapped in the cylinder,
 501 Equation 1.

$$IAR = \frac{m_{air_HP}}{m_{air_HP} + m_{air_LP_trapped}} \quad (1)$$

502 In Figure 15, some key engine parameters, as BSFC, $\sigma IMEP$ and com-
 503 bustion efficiency (calculated from the measured CO and UHC content in
 504 the exhaust gases), are plotted vs. the IAR for all the operating conditions
 505 analyzed in this paper (see Figure 7). It is important to remark that, whereas
 506 the values of $\sigma IMEP$ and combustion efficiency are comparable among the

507 different operating points, this is not the case for the BSFC. For this reason,
 508 this last parameter has been normalized (with a linear transformation), to
 509 make it comparable among all the operating points, but (of course!) keeping
 510 the trends of the parameter. The following observations can be done:

- 511 • For each parameter, all the operating points show a similar trend, which
 512 is indicated by a dashed red line.
- 513 • For a value of IAR of around 0.09, all three parameters are optimized
 514 at the same time: BSFC is minimum (maximum fuel efficiency), the
 515 IMEP variability is minimum (maximum stability) and the combustion
 516 efficiency is maximum.

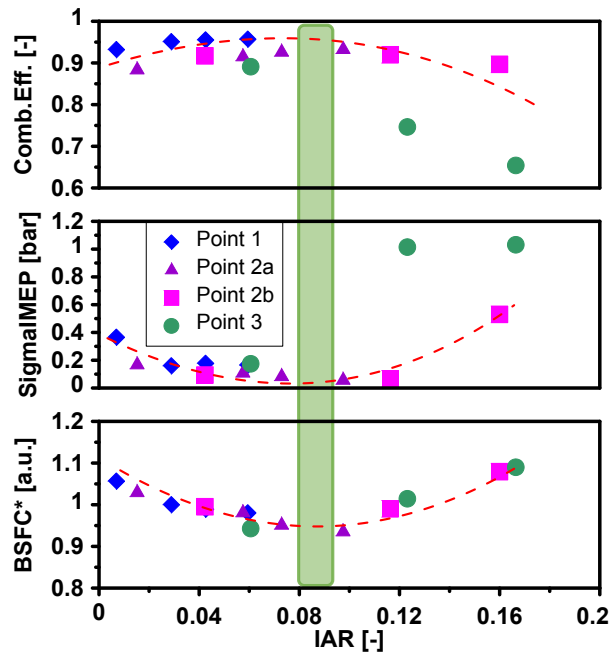


Figure 15: Effect of the IAR on BSFC, $\sigma IMEP$ and combustion efficiency.

517 This result indicates that, for each operating condition (engine speed and
518 load) there is an optimum value of the DOI to optimize the engine behavior.

519 *3.4. Influence of EGR on the combustion process*

520 With the current engine and its controlling parameters presented up to
521 now, its performance in some standard cycles has been evaluated using the
522 methodology already presented in subsection 2.3 (results shown in Table 1).
523 Based on these estimations, it can be seen that, without any particular tech-
524 nique to reduce NO_x emissions, this engine would be able to fulfill the Bharat
525 standards, currently in force in an emerging country, which is significantly less
526 demanding than in any other more developed country. But for the progress
527 of the engine design, and to allow its application in more stringent scenarios,
528 it is compulsory to include some NO_x reduction strategy. As already said
529 before, an EGR system will be implemented to allow further reductions in
530 NO_x emissions. The reason for choosing an EGR system instead of an ex-
531 haust after-treatment system (an SCR, for example) is, among others, the
532 advantage to win another control parameter for the engine operation. In fact,
533 the effect of introducing EGR on the combustion process and its control is
534 what will be analyzed now.

535 The EGR introduction affects in different ways the engine performance
536 depending on the operating point. Therefore, the results will be presented
537 divided in the different engine loads, as in the previous sections.

538 *3.4.1. High load*

539 At high load operation, an increase in the equivalence ratio leads to a
540 limitation in the CA50 advance due to knock, since the reactivity of the

Cycle	Fuel cons. l/100km	NO_x mg/km	NO_x Limit mg/km
Bharat	3.58	82.0	80
NEDC	3.87	209.2	60
WLTP	3.85	298.5	60

Table 1: Results from the performance of a vehicle powered by the engine without EGR in 3 different standard cycles.

541 mixture is increased. This effect prevents the correct positioning of the com-
542 bustion event in the cycle. In this context, thanks to the EGR introduction
543 the knock is mitigated and, thus, the combustion can be further advanced
544 (Figure 16 to the right). This leads to an improvement in BSFC despite
545 the loss in combustion efficiency associated to the lower O_2 content in the
546 intake gases caused by the EGR introduction (see Figure 16 to the left): fuel
547 consumption is improved in 2.3% even assuming a loss of 4% in combustion
548 efficiency, and NO_x emissions are reduced in 75.6%. These results show the
549 strong potential of EGR to reduce NO_x , which is a more than usual result.
550 But, at the same time, EGR also serves to improve BSFC, because of its
551 knock mitigation capability. This capability will be further analyzed in the
552 following paragraphs.

553 Figures 17 and 18 show a cycle-to-cycle analysis from a tested point with
554 the same configuration as before ($Fr=0.75$), where the spark advance and
555 the EGR rate are modified, respectively, in order to advance the combustion
556 position (i.e., the CA50). These two figures include two graphs in both cases:
557 the main graph shows the instantaneous MAPO (which quantifies knock and

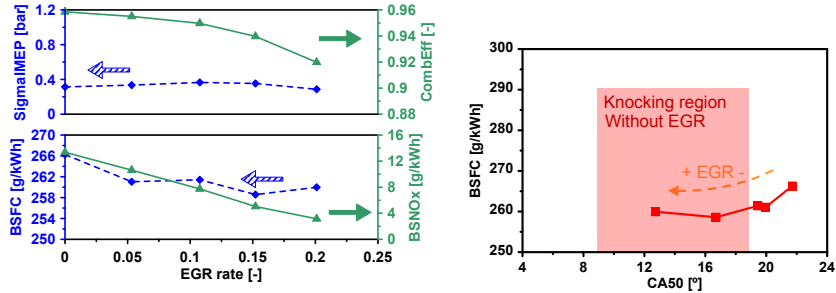


Figure 16: Point 1. High equivalence ratio case ($Fr=0.75$). Evolution of different parameters as a function of the EGR rate (**left**). For the same tests, correlation between BSFC and CA50, and detail of the knocking region when no EGR is used (**right**).

558 was defined in section 2.3) for each measured cycle (250 cycles per test) vs.
 559 the corresponding CA50, whereas the sub-graph shows the same information
 560 but averaged (MAPO mean vs. CA50 mean). The first case (Figure 17)
 561 shows an attempt to advance the combustion position without EGR, only
 562 advancing the spark timing. As can be seen, in this case the MAPO increases
 563 with the combustion advance (CA50), as expected.

564 However, in Figure 18, the combustion process, for the same operating
 565 point in similar conditions ($Fr=0.8$), is advanced by the introduction of a
 566 15% EGR rate. The result is an advance of the combustion process without
 567 any significant change in knock (in fact, the mean value of the MAPO is even
 568 slightly lower than in the starting point). This result illustrates the strong
 569 potential of EGR to mitigate knock, thus allowing significant improvements
 570 in terms of fuel economy [24] and NO_x emissions.

571 Still at high load, but with lower equivalence ratios (Figure 19), where
 572 knock is not a problem for the correct combustion positioning, the introduc-
 573 tion of EGR does not bring the clear benefit seen before, since the combustion

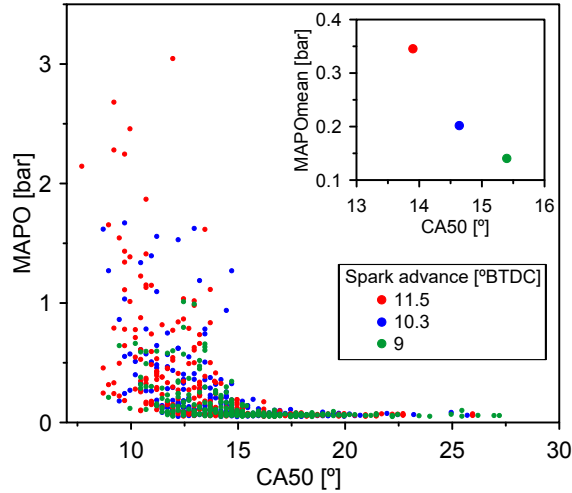


Figure 17: MAPO vs. CA50 for all individual cycles (main graph) or averaged (detailed graph) for a spark timing swept.

574 onset is placed even too early in the cycle. Thus, in this other case, the NO_x
 575 reduction is attained at the expense of an increase in BSFC. This BSFC de-
 576 terioration can be explained as follows: the dilution effect of the mixture and
 577 the reactivity loss, both caused by EGR, lead to a decrease in combustion
 578 stability that needs to be compensated by an advanced spark timing (CA50 is
 579 placed too early) to hold a stable enough combustion process. This, coupled
 580 to the deterioration in combustion efficiency, leads to a significant increase
 581 in BSFC.

582 Given the widely-known NO_x reduction effect of EGR and all the previous
 583 explained effects, it is found that, at high loads, the EGR strategy improves
 584 considerably the NO_x -BSFC trade-off (shown in Figure 20). In view of this
 585 figure, it can be stated that NO_x emissions can be reduced in a factor of 4
 586 without any increase in BSFC, or even slightly improving it.

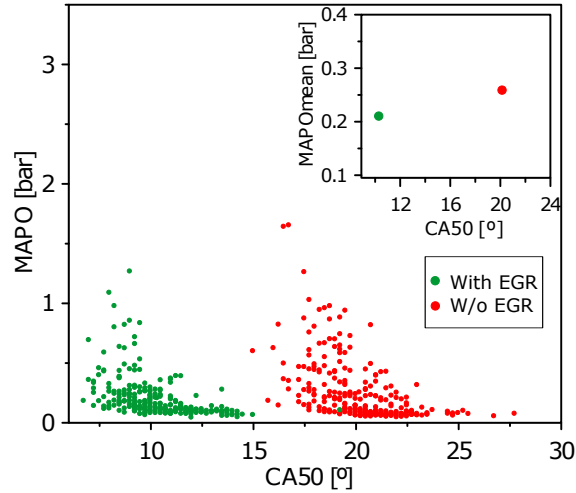


Figure 18: MAPO vs. CA50 for all individual cycles (main graph) or averaged (detailed graph), for two different cases: with (green) and without EGR (red).

587 *3.4.2. Medium and low load*

588 As far as the engine load is reduced, the limitation in CA50 position
 589 caused by knock disappears. Besides, in contrast with the previous scenario,
 590 because the combustion mode switches to CAI mode, the spark timing loses
 591 its controlling capability over the combustion process. Thus, now the CA50
 592 can be correctly positioned by some means (e.g. Fr and/or VVT position,
 593 not the spark timing) other than EGR. Consequently, the role of EGR in
 594 this other scenario will be less important.

595 As in the previous subsection, the effect of the EGR will be analyzed at
 596 two different Fr's. In Figure 21, to the left, the evolution of different engine
 597 parameters as a function of the EGR rate is presented, for Point 2b (see
 598 Figure 7) at low Fr (0.65). The trends are similar to the ones already seen
 599 in the previous subsection, for higher loads. The following comments can be

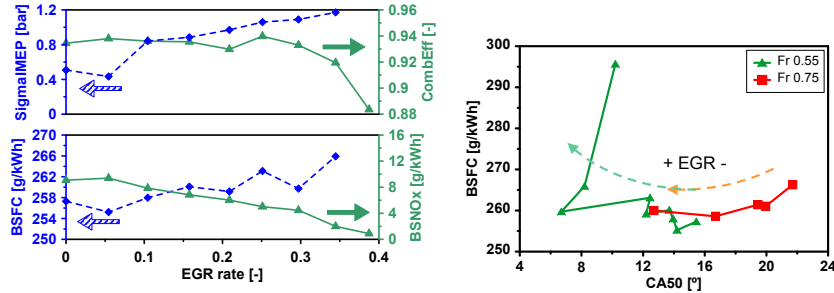


Figure 19: Point 1. Low equivalence ratio case ($Fr=0.55$). Evolution of different parameters as a function of the EGR rate (**left**). For the same tests, correlation between BSFC and CA50. In this case, the results for the $Fr=0.75$ case are also shown (**right**).

600 done:

- 601 • EGR significantly reduces NO_x emissions. However, the starting levels
- 602 of NO_x are already low, and the use of EGR is much less justified than
- 603 at higher loads. Remember that at CAI operating mode, the IGR rate
- 604 is significantly high, and NO_x emissions are naturally low.

- 605 • BSFC worsens with EGR. On the one hand, as observed in Figure 21,
- 606 to the right, this is because the combustion process is delayed (CA50
- 607 moves away from TDC). The reason for this is the lower reactivity of
- 608 the in-cylinder mixture, and cannot be compensated with the spark
- 609 timing, since it does not control the combustion onset anymore. On
- 610 the other hand, this is also the result of the loss in combustion efficiency
- 611 caused by EGR that can be observed in the figure as well.

- 612 • The lower mixture reactivity also explains the decrease in combustion
- 613 efficiency, as well as the increase in $\sigma IMEP$ (the engine is more un-
- 614 stable).

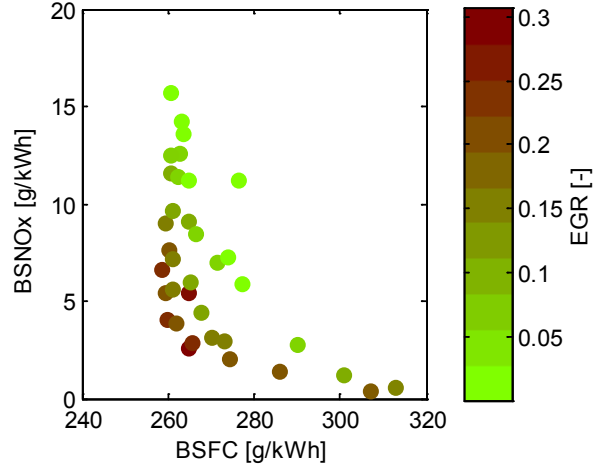


Figure 20: NO_x -BSFC trade-off. The color scale gives information about the EGR rate.

615 For higher Fr 's (e.g. 0.75 in 21), because of the higher mixture reactivity,
 616 the combustion onset takes place too early, and the engine operates in the
 617 non-interesting region shaded in the figure to the right. The operation in
 618 this region needs to be avoided because, depending on the operating point,
 619 either the combustion onset is placed too early or some knock can appear.
 620 In this other case, EGR can help to place the combustion onset on the right
 621 place, as shown in Figure 21 to the right, thus allowing to meet, together,
 622 lower NO_x and BSFC.

623 Therefore, at the operating points where the combustion process was
 624 already well placed in the cycle, EGR only serves to reduce NO_x emissions.
 625 But taking into account the initially low NO_x emissions because of the CAI
 626 combustion, it might be not necessary to add EGR in most cases.

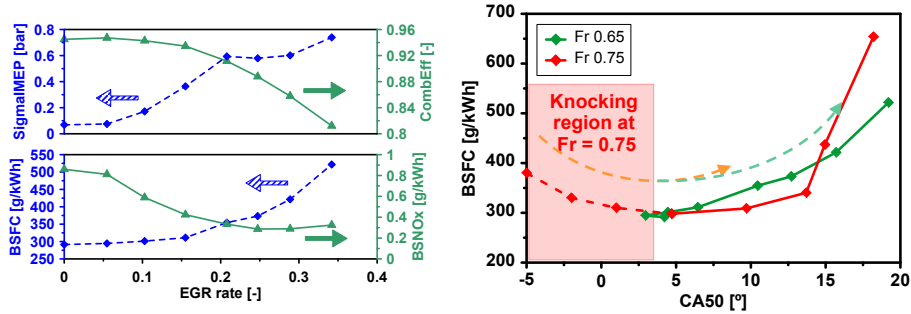


Figure 21: Point 2b. Low equivalence ratio case ($Fr=0.65$). Evolution of different parameters as a function of the EGR rate (**left**). For the same tests, correlation between BSFC and CA50. In this case, the results for a higher Fr ($Fr=0.75$) case are also shown (**right**).

627 As a conclusion, the use of EGR, as well as reducing NO_x emissions,
 628 allows the exploration of operating points that were previously impossible
 629 to achieve due to the excessively high knock level or the too early combus-
 630 tion onset. At the operating points where the excessive mixture reactivity
 631 represents a problem for the point optimization, the introduction of EGR
 632 decreases this reactivity and allows the correct combustion positioning, thus
 633 improving the fuel efficiency with a lower level of NO_x emissions. With this
 634 new degree of freedom in the engine, a wider range is now available at each
 635 operating point to look for lower NO_x together with the same or even lower
 636 BSFC. Besides, even the engine peak power can be increased (based on some
 637 other results not presented here, the increase in peak power can be around
 638 25%).

639 Last, the results of the estimated performance of the engine, but now with
 640 an EGR system, on the different standard cycles has been reviewed, and they
 641 are shown in Table 2. Now, even the most stringent standards are fulfilled
 642 in terms of NO_x , even if the overall fuel consumption has increased respect

643 to the cases already shown in Table 1. This is a proof of the potential of this
 644 engine concept to be applied even in the most stringent markets, where it
 645 can help to reduce CO_2 emissions respect to the use of standard 4S gasoline
 646 engines.

Cycle	Fuel cons. l/100km	NO_x mg/km	NO_x Limit mg/km
Bharat	4.18	30.8	80
NEDC	4.47	47.5	60
WLTP	4.38	52.8	60

Table 2: Results from the performance of a vehicle powered by the engine with EGR in 3 different standard cycles, to be compared to those without EGR already presented in Table 1.

647 4. Conclusions

648 The present engine, as shown along the whole paper, has several charac-
 649 teristics that make it unique. Its capability to operate in different combustion
 650 modes together with the fact of being a 2S engine, make it much more com-
 651 plex (in terms of operation, but not of cost) than any traditional 4S engine.
 652 First, the IGR control (hot residual trapped gases) plays a fundamental role,
 653 since it strongly affects the mixture reactivity. Depending on the operating
 654 conditions, a high IGR rate will be interesting to achieve a CAI combustion
 655 mode, or, on the contrary, when the autoignition of the mixture can be dan-
 656 gerous for the engine mechanical integrity (knock), the IGR rate needs to be
 657 minimized to allow the correct placement of the combustion onset without
 658 any autoignition of the mixture.

659 The autoignition conditions are mainly controlled by means of the equiv-
660 alence ratio, which has two effects that go in the same direction: on the one
661 hand, it affects the mixture reactivity by changing the fuel/air ratio but, on
662 the other hand, it also affects the IGR ratio. Remember that, for a given
663 operating point, the mass of fuel is fixed, and the equivalence ratio is mod-
664 ified by changing the amount of air: more air (i.e. lower Fr) means less
665 IGR, both leading to a lower mixture reactivity; and, on the contrary, less
666 air (i.e. higher Fr) means more IGR, both leading to a higher mixture re-
667 activity. Additionally, with the EVC modification, the effective compression
668 and expansion strokes can be modified. This modification allows the cor-
669 rect adjustment of the combustion location in the cycle when the operating
670 points are in CAI mode, or it can reduce the knock intensity when operat-
671 ing in SI mode, since this change affects the thermal in-cylinder conditions
672 (temperature and pressure).

673 Regarding the injection parameters, on the one hand, advanced SOI's
674 seem to optimize the engine behavior in most operating conditions. On the
675 other hand, an optimum relationship between the air mass flow introduced
676 through the injection system and the one introduced through the intake has
677 been found, which is the key factor to find the optimum DOI.

678 Finally, in relation to the use of EGR, besides of decreasing the NO_x
679 emissions, it has also revealed to be a key parameter to control the combus-
680 tion process at high loads. With EGR, the knock can be mitigated thanks to
681 the loss in mixture reactivity, introducing the possibility to operate in new
682 conditions (where the operation was previously impossible) and giving the
683 opportunity to get better fuel efficiency. Furthermore, an additional benefit

684 of this strategy can be, on the one hand, the decrease of the maximum air
685 mass flow (due to the increase of the Fr at high load), which allows a reduc-
686 tion in the blower requirements and, with this, a general reduction in fuel
687 consumption; and, on the other hand, for the same maximum air mass flow,
688 to increase the engine peak power (up to around 25%).

689 Throughout all the present research, this engine concept has shown its
690 big potential. In emerging markets (e.g. India), it can fulfill the emissions
691 levels without any particular device or strategy to reduce NO_x , thanks to
692 the advantages of the CAI combustion mode, thus being a really low cost
693 solution in this scenario. And in more stringent markets, with the introduc-
694 tion of an EGR system (which implies the use of a particulate filter), also
695 the corresponding standards can be fulfilled. In this other case, the concept
696 can be still attractive from the economical point of view, especially when
697 compared to other solutions with more expensive systems (SCR or similar),
698 and also from the point of view of CO_2 reduction compared to more standard
699 4S gasoline engines.

700 **Acknowledgments**

701 The authors would like to thank different members of the CMT-Motores
702 Térmicos team of the Universitat Politècnica de València for their contri-
703 bution to this work. The authors would also like to thank the Universitat
704 Politècnica de València for financing the PhD. studies of Jorge Valero-Marco
705 (contract 3102). This work was partly funded by Renault S.A.S., the con-
706 tribution of which is greatly acknowledged, and by FEDER and the Spanish
707 Government through project TRA2015-67136-R.

708 **Notation**

2S	Two Stroke
4S	Four Stroke
ATDC	After Top Dead Center
BDC	Bottom Dead Center
BSFC	Brake Specific Fuel Consumption [g/kWh]
BSNO _x	Brake Specific NO_x emissions [g/kWh]
BTDC	Before Top Dead Center
CA50	Crank Angle where 50% of the fuel mass has been burned
CA75	Crank Angle where 75% of the fuel mass has been burned
CAI	Controlled AutoIgnition
DOI	Duration Of Injection (air + fuel injection)
709 EGR	External Gas Recirculation
EOI	End Of Injection (air + fuel injection)
EVC	Exhaust Valve Closing
Fr	Fuel/air equivalence Ratio
HRR	Heat Release Rate
IAR	Injected Air Ratio (ratio between the injected air and the total trapped air)
IGR	Internal Gas Recirculation (i.e. residual gases)
IMEP	Indicated Mean Effective Pressure
MAPO	Maximum Amplitude of Pressure Oscillations
MBT	Maximum Brake Torque

	NEDC	New European Driving Cycle
	SCR	Selective Catalytic Reduction
	SOI	Start Of Injection (air + fuel injection)
710	TDC	Top Dead Center
	VVA	Variable Valve Actuation
	VVT	Variable Valve Timing
	WLTP	Worldwide harmonized Light vehicles Test Procedure

711 **Appendix A. Appendix A: effect of IGR on the ignition delay**

712 In this appendix the ignition delay of a mixture of air + IGR wants to
713 be assessed as a measure of its knocking tendency. The motivation is to find
714 out which effect is stronger: the effect of the oxygen content reduction when
715 the IGR rate increases, which would reduce the mixture reactivity; or the
716 effect of the increase in mixture temperature when the IGR increases, which
717 would increase the mixture reactivity.

718 For the study, the following hypotheses and assumptions were taken:

- 719 • The air in the intake manifold is at 323 K. This is assumed to be the
720 initial temperature of the air trapped in the cylinder.
- 721 • The exhaust gases in the exhaust manifold are at 827 K. This is also as-
722 sumed to be the initial temperature of the residual gases (IGR) trapped
723 in the cylinder.
- 724 • With the two previous assumptions, the initial temperature of the mix-
725 ture is calculated, as a function of the IGR rate, taking into account
726 the c_p , initial temperature and mass fraction of both air and IGR.

- 727 • The mixture at known initial conditions is assumed to be compressed
728 up to TDC (consequently both the temperature and pressure are sig-
729 nificantly increased), and then introduced in a PSR (Perfectly Stirred
730 Reactor) reactor (i.e. a perfectly homogeneous reactor), where the au-
731 toignition process is going to be studied with Chemkin. It is worthy
732 to note that the compression up to TDC is necessary to ensure the
733 mixture autoignition.
- 734 • The ignition delay is considered to happen when 50% of the total tem-
735 perature increase in the reactor takes place.
- 736 • The fuel considered was iso-octane (the chemical mechanism considered
737 was that from Curran et al. [25]), and the equivalence fuel/air ratio was
738 1 (for $Fr=0.6$, it was checked that the conclusions are exactly the same).

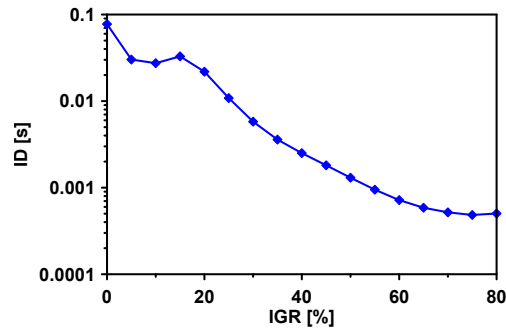


Figure A.22: Effect of the IGR rate on the ignition delay.

739 The results of the simulations are presented in Figure A.22. It can be seen
740 that, in the main range of IGR rates, the higher the IGR rate, the lower the
741 ignition delay, meaning that the thermal effect is stronger than the dilution

742 effect. This trend is clearly broken at very high IGR rates (above 75%; for
743 an $Fr=0.6$, this shift in the trend takes place at an IGR rate of 90%), and
744 at low IGR rates (below 15%). It should be taken into account, however,
745 that the minimum IGR rate achievable in the engine is between 10 to 15%,
746 whereas the maximum IGR rate is between 80 to 90%. Consequently, in the
747 possible range of IGR allowed in the engine, the higher the IGR, the higher
748 the mixture reactivity.

749 References

- 750 [1] S. Barclay. Lotus omnivore engine - 10% better fuel economy than
751 current leading gasoline engines. *Automotive Industries AI*, 189(12),
752 2009.
- 753 [2] M. Nuti. Direct fuel injection: An opportunity for two-stroke si engines
754 in road vehicle use. *SAE Technical Paper 860170*, 1986.
- 755 [3] M. M. Rahman, A. K. Ariffin, S. Abdullah, M. M. Noor, and A. B. Rosli.
756 Durability assessment of cylinder block for two stroke free piston linear
757 engine using random loading. *American Journal of Applied Sciences*,
758 6(4):726–735, 2009.
- 759 [4] G. A. Lustgarten and K. Aeberli. Improved liner and ring wear proper-
760 ties of two-stroke diesels. *Diesel and Gas Turbine Worldwide*, 20(3):45–
761 48, 1988.
- 762 [5] O. A. Kutlar, H. Arslan, and A. T. Calik. Methods to improve efficiency
763 of four stroke, spark ignition engines at part load. *Energy Conversion*
764 *and Management*, 46(20):3202–3220, 2005.

- 765 [6] H. Zhao. *HCCI and CAI Engines for the Automotive Industry*. Wood-
766 head Publishing Limited, 2007.
- 767 [7] Y. Zhang and H. Zhao. Investigation of combustion, performance
768 and emission characteristics of 2-stroke and 4-stroke spark ignition and
769 cai/hcci operations in a di gasoline. *Applied Energy*, 130:244–255, 2014.
- 770 [8] S. Onishi, S. H. Jo, K. Shoda, P. D. Jo, and S. Kato. Active thermo-
771 atmosphere combustion (atac) - a new combustion process for internal
772 combustion engines. *SAE Technical Paper 790501*, 1979.
- 773 [9] M. Noguchi, Y. Tanaka, T. Tanaka, and Y. Takeuchi. A study on gaso-
774 line engine combustion by observation of intermediate reactive products
775 during combustion. *SAE Technical Paper 790840*, 1979.
- 776 [10] D. Flowers, S. Aceves, R. Smith, J. Torres, J. Girard, and R. Dibble.
777 Hcci in a cfr engine: Experiments and detailed kinetic modeling. *SAE*
778 *Technical Paper 2000-01-0328*, 2000.
- 779 [11] A. C. Alkidas. Combustion advancements in gasoline engines. *Energy*
780 *Conversion and Management*, 48(11):2751–2761, 2007.
- 781 [12] C. H. Lee and K. H. Lee. An experimental study of the combustion
782 characteristics in scci and cai based on direct-injection gasoline engine.
783 *Experimental Thermal and Fluid Science*, 31(8):1121–1132, 2007.
- 784 [13] E. Sigurdsson, K. M. Ingvorsen, M. V. Jensen, S. Mayer, S. Matlok, and
785 J. H. Walther. Numerical analysis of the scavenge flow and convective
786 heat transfer in large two-stroke marine diesel engines. *Applied Energy*,
787 123:37–46, 2014.

- 788 [14] K. M. Pang, N. Karvounis, J. H. Walther, and J. Schramm. Numerical
789 investigation of soot formation and oxidation processes under large two-
790 stroke marine diesel engine-like conditions using integrated cfd-chemical
791 kinetics. *Applied Energy*, 169:874–887, 2016.
- 792 [15] E. Mattarelli, C. A. Rinaldini, and M. Wilksch. 2-stroke high speed
793 diesel engines for light aircraft. *SAE International Journal of Engines*,
794 4(2):2338–2360, 2011.
- 795 [16] M. I. Lamas and C. G. Rodríguez Vidal. Computational fluid dynamics
796 analysis of the scavenging process in the MAN B&M 7S50MC two-stroke
797 marine diesel engine. *Journal of Ship Research*, 56(3):154–161, 2012.
- 798 [17] J. Benajes, R. Novella, D. De Lima, P. Tribotté, N. Quechon, P. Ober-
799 nesser, and V. Dugue. Analysis of the combustion process, pollutant
800 emissions and efficiency of an innovative 2-stroke hsdie engine designed
801 for automotive applications. *Applied Thermal Engineering*, 58(1-2):181–
802 193, 2013.
- 803 [18] M. Lapuerta, O. Armas, and J. J. Hernández. Diagnosis of diesel com-
804 bustion from in-cylinder pressure signal by estimation of mean thermo-
805 dynamic properties of the gas. *Applied Thermal Engineering*, 19(5):513–
806 529, 1999.
- 807 [19] M. Lapuerta, O. Armas, and V. Bermúdez. Sensitivity of diesel engine
808 thermodynamic cycle calculation to measurement errors and estimated
809 parameters. *Applied Thermal Engineering*, 20(9):843–861, 2000.

- 810 [20] X. Zhen, Y. Wang, S. Xu, Y. Zhu, C. Tao, T. Xu, and M. Song. The
811 engine knock analysis - an overview. *Applied Energy*, 92:628–636, 2012.
- 812 [21] J. J. Lopez, R. Novella, J. Valero-Marco, G. Coma, and F. Justet. Eval-
813 uation of the potential benefits of an automotive, gasoline, 2-stroke en-
814 gine. *SAE Technical Paper 2015-01-1261*, 2015.
- 815 [22] J. Benajes, J. J. Lopez, J. Valero-Marco, G. Coma, and F. Justet. Design
816 and evaluation of an automotive, low cost, gasoline, 2-stroke engine. In
817 *The low CO₂ spark ignition engine of the future and its hybridization*,
818 *SIA Powertrain Versailles*. SIA, Société des Ingénieurs de l’Automobile,
819 2015.
- 820 [23] J. Benajes, J. J. Lopez, J. Valero-Marco, G. Coma, and C. Libert. Tran-
821 sition between si and cai operating modes in an automotive, low cost,
822 gasoline, 2-stroke engine. In *The low CO₂ spark ignition engine of the*
823 *future and its hybridization, SIA Powertrain Versailles*. SIA, Société des
824 Ingénieurs de l’Automobile, 2017.
- 825 [24] J.M. Luján, H. Climent, R. Novella, and M.E. Rivas-Perea. Influence
826 of a low pressure egr loop on a gasoline turbocharged direct injection
827 engine. *Applied Thermal Engineering*, 89(5):432–443, 2015.
- 828 [25] H.J. Curran, P. Gaffuri, W.J. Pitz, and C.K. Westbrook. A comprehen-
829 sive modeling study of iso-octane oxidation. *Combustion and Flame*,
830 129(3):253–280, 2002.